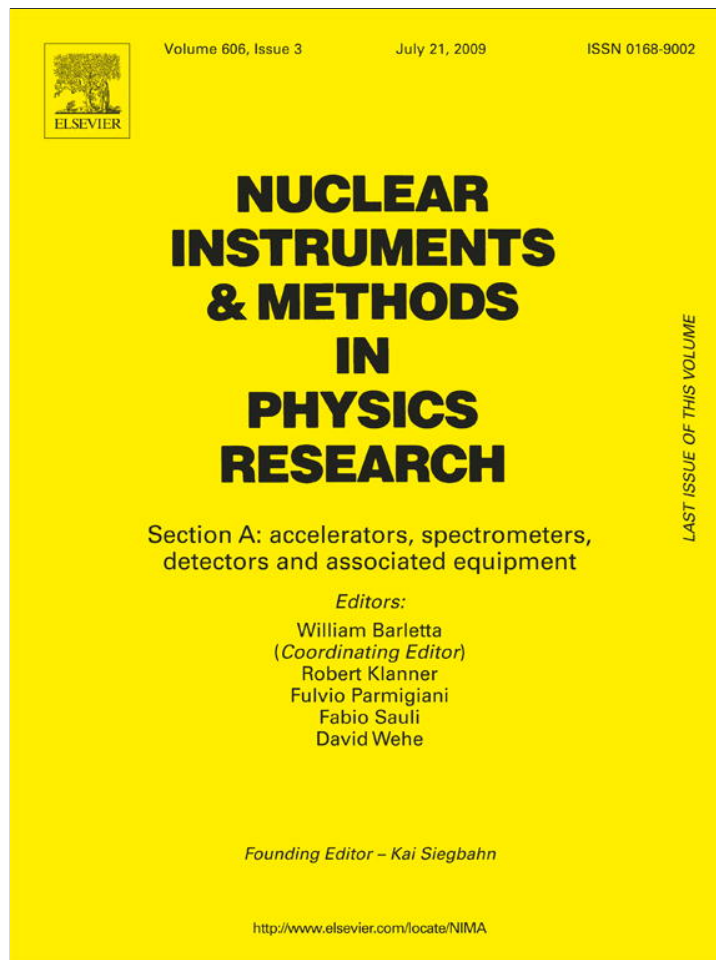


Provided for non-commercial research and education use.  
Not for reproduction, distribution or commercial use.



This article appeared in a journal published by Elsevier. The attached copy is furnished to the author for internal non-commercial research and education use, including for instruction at the authors institution and sharing with colleagues.

Other uses, including reproduction and distribution, or selling or licensing copies, or posting to personal, institutional or third party websites are prohibited.

In most cases authors are permitted to post their version of the article (e.g. in Word or Tex form) to their personal website or institutional repository. Authors requiring further information regarding Elsevier's archiving and manuscript policies are encouraged to visit:

<http://www.elsevier.com/copyright>



Contents lists available at ScienceDirect

# Nuclear Instruments and Methods in Physics Research A

journal homepage: [www.elsevier.com/locate/nima](http://www.elsevier.com/locate/nima)

## Investigation of the energy accumulation rate in solid deuterium irradiated with fast electrons

D. Bondoux<sup>a</sup>, H.G. Börner<sup>a</sup>, V. Ermilov<sup>b</sup>, J.P. Gonzales<sup>a</sup>, E. Kulagin<sup>b</sup>, S. Kulikov<sup>b</sup>, E. Lelievre-Berna<sup>a</sup>, V. Melikhov<sup>b</sup>, V.V. Nesvizhevsky<sup>a,\*</sup>, T. Soldner<sup>a</sup>, F. Thomas<sup>a</sup>, E. Shabalin<sup>b</sup>

<sup>a</sup> Institut Laue-Langevin, 6 rue Jules Horowitz, 38042 Grenoble, France

<sup>b</sup> Joint Institute for Nuclear Research, Dubna, Russia

### ARTICLE INFO

#### Article history:

Received 21 December 2007

Received in revised form

30 March 2009

Accepted 5 April 2009

Available online 3 May 2009

#### Keywords:

Ultracold neutrons

Neutron sources

### ABSTRACT

The feasibility studies for a new ultra cold neutron (UCN) source to be installed at the Institut Laue-Langevin (ILL) are underway. One of these studies concerns a source using solid deuterium (SD<sub>2</sub>) as a neutron moderator. During source operation the SD<sub>2</sub> would be exposed to intense  $\gamma$ -ray and neutron fluxes. These may result in radiolysis in SD<sub>2</sub>. Our work has shown that this effect—if it is produced—is not incompatible with a normal operation of the source.

© 2009 Elsevier B.V. All rights reserved.

### 1. Introduction

The so-called “burps” in solid-ice samples could occur under irradiation with  $\gamma$ -quanta, electrons, and fast neutrons [1–4]. They have been observed in a number of hydrogen-containing materials (for instance, in ice and solid methane). In these processes, molecules of the ice material are destroyed and the energy of the resulting free radicals accumulates. This energy can be released suddenly as the radicals recombine. The result can be a significant and violent increase in the temperature of the sample. This possibility has to be taken into account when considering the feasibility of SD<sub>2</sub> UCN sources [5–23]. If such a phenomenon occurs in SD<sub>2</sub>, it might limit the time where the converter can be kept at low temperature. This could necessitate a periodical regeneration of the converter. In the worst case, this might even cause “burps” which could destroy the converter and/or even the source.

In fact, such stored energy effects had already been investigated for SD<sub>2</sub> and SH<sub>2</sub> samples irradiated by electrons, protons, and  $\gamma$ -quanta [24–31]. The energy from incoming 3 keV electron and 10 keV ion beams, partially absorbed in SH<sub>2</sub> and SD<sub>2</sub> samples at temperatures of 2.5–3 K, was studied in [24]. A phenomenological rate process theory was developed in [25] to explain the storage and rapid recombination of atomic-hydrogen radicals in crystalline molecular hydrogen solid at temperatures in the range  $0.1\text{ K} \leq T \leq 4\text{ K}$ . It quantitatively described the observed storage

time as a function of temperature in many cases. This model can also be applied to SD<sub>2</sub>. The infrared absorption spectrum of SD<sub>2</sub> at 4.2 K was studied with a sample irradiated by a 15 MeV proton beam [26]. Comparison of the beam-induced spectral features with those previously seen in a tritium-doped sample conclusively established the presence of a radiation-induced absorption process. After turning off the proton beam, these features persisted for the order of hours. They could be quenched by heating the sample to  $\sim 11\text{ K}$ . Charge-induced absorption spectra in the fundamental band of SD<sub>2</sub>—under proton-beam irradiation—were measured in [27]. The timing experiments were presented there, in which the growth and decay of these spectral features are monitored following the onset and termination of beam irradiation. Both spectra and timing as a function of temperature were examined. In [28], electron-spin-resonance (ESR) spectra of H (D) atoms, produced in  $\gamma$ -irradiated SH<sub>2</sub> were studied at 4.2 K. The ESR linewidth of the trapped hydrogen atoms depends significantly upon the matrices of hydrogen isotopes. The ESR linewidth has been calculated with the orthogonalized wavefunction on the basis of the model presented. It is concluded from the comparison of the experimental ESR linewidth with theoretical ones that H atoms in solid H<sub>2</sub> are trapped in substitution sites, while H (D) atoms in solid HD and SD<sub>2</sub> are trapped in interstitial octahedral sites. In [29], the authors measured the isothermal build-up of the atomic-hydrogen (T and D) concentrations inside ST<sub>2</sub> and D–T from 1.3 to 10 K. The atoms are produced by the  $\beta$  decay of tritium. The measurements were made using adiabatic slow-passage ESR techniques. The atom concentration increases with time and with decreasing temperature; it reaches 0.2% below 3 K. In [30],

\* Corresponding author. Tel.: +33 4762 077 95; fax: +33 4762 077 77.  
E-mail address: nesvizhevsky@ill.eu (V.V. Nesvizhevsky).

samples of  $SD_2$ , cooled below 4.2 K, and irradiated by 15 MeV protons, spontaneously flashed. The flash spectrum occurred in the near infrared with a maximum close to 920 nm. The flash intensity was two to three orders of magnitude greater than a steady-state emission observed in the same spectral region. The flash frequency was 1 every 1 to 3 min after several hours of irradiation of  $10 \text{ nA/cm}^2$ . The heat pulses were detected accompanying many of the flashes and both can be stimulated by the application of external heat triggers. Following the optical flash, the steady-state emission intensity decreased by an amount that is wavelength dependent. While it is thought that these flashes are caused by atomic association in the solid, the species responsible for the optical emission and the transition are uncertain. Finally, optical emission from proton-beam-irradiated  $SD_2$  was studied in [31] after termination of the proton beam. The continuous red emission showed a residual intensity that persisted over 30 min from termination of the beam. Optical flashes can also be thermally triggered over 10 min after termination of irradiation. Such triggered flashes were shown to quench the infrared absorption of Stark-shifted charge-induced features. Ultraviolet photons can stimulate this red emission after termination of irradiation with no measurable decrease in intensity for 40 min.

Although much data is available on comparable systems and some predictions for a  $SD_2$  moderator can be deduced, the straight experimental test on a pure  $D_2$  sample under representative irradiation has been missing. The closest full-scale test to the realistic Institut Laue-Langevin (ILL) conditions was probably carried out in Ref. [9] with 6 l of  $SD_2$  installed in the PNPI reactor in Gatchina. However, the temperature was too high: 8–10 K instead of 5–6 K required; the heat load was too low; 0.03–0.05 W/g instead of a few tenths W/g required. No “burps” were observed under these conditions but this does not yet prove that this phenomenon—if it is produced—is compatible with a normal operation of the source.

In order to achieve maximum UCN density, we have to keep the source temperature low, at 5–6 K. Under the intense radiation inside the reactor the  $D_2$  molecules decompose into D-atoms. At low temperatures the diffusion of D-atoms is very slow; the recombination might therefore also be slow. This would result in the accumulation of radicals. In this case, as the  $SD_2$  heats, there is the possibility of a fast chain reaction leading to the recombination of D-atoms and a subsequent sudden increase in temperature. If the energy released exceeds 55 J/mole, any  $SD_2$  sample would start to melt. The effect of such a rapid recombination of free radicals in  $SD_2$  has never been directly measured. This is the reason underlying the present work. An adequate understanding of this process is essential for the construction of any  $SD_2$  source in the world. It is particularly important for the ILL, given the powerful fluxes of cold neutrons and  $\gamma$ -quanta at the future source position (see Fig. 1).

Such a UCN source would be in line with the Munich project [10]. There, the UCN density is accumulated in a neutron guide or in a storage volume with low wall losses. UCN are produced in small volume solid-deuterium source placed in maximum flux of cold neutrons. In contrast to that, the ILL project would differ by new technology available, by additional constraints and advantages of its reactor, as well as by specific criteria for the optimization of our source: We would take advantage of specular neutron guides with nearly ideal transmission of neutrons at specular trajectories [32–34]. Long specular neutron guides of limited cross-section would be useful, in particular keeping in mind many geometrical constraints at the existing ILL reactor. In case of an installation of a third cold neutron source at the ILL, we would profit from higher initial density of cold neutrons in its vicinity. Otherwise a dedicated cold neutron converter around a

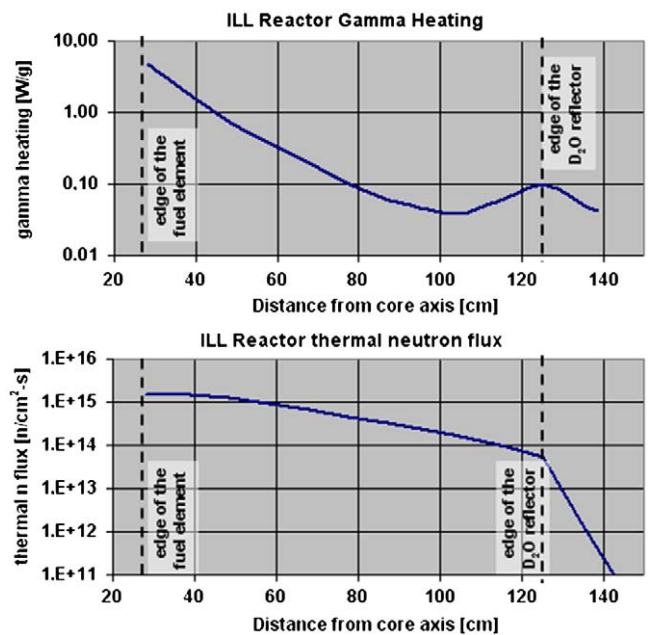


Fig. 1.  $\gamma$ -heating and thermal neutron flux in the ILL reactor. A possible distance of a  $SD_2$  source from the core is 50–80 cm.

$SD_2$  UCN source would be needed. Anyway a  $SD_2$  UCN source has to be placed in maximum flux of cold neutrons. We would also optimize our source for maximum brightness/density against the total flux of produced neutrons, keeping in mind such brightness-demanding projects as, for instance, the resonance transitions of neutrons between the gravitationally bound quantum states [35,36].

## 2. Tentative source at the ILL

No decision has been taken so far concerning the construction of a  $SD_2$  UCN source at the ILL. Therefore, we will present only approximate parameters, leaving any detailed study for the future. The deuterium converter is installed in the vicinity of the reactor core, in a very high  $\gamma$ -flux (see Fig. 1). It has to be cooled down to a few Kelvin temperatures using liquid helium. In order to minimize the required helium flow, the heating load to be evacuated (i.e. the total mass to be cooled) has to be as small as possible. We studied various exchanger geometries and materials and favoured the configuration as shown in Fig. 2.

The heat exchanger shape is shown in Fig. 2 on the right. The heat exchanger is cooled by helium flow between the two plates. Deuterium is frozen on its cold surface from deuterium gas around the converter. Deuterium gas is injected directly into the neutron guide.

The choice of the exchanger material is constrained by the following criteria: (1) high critical velocity in order to allow storage of UCN, (2) high thermal conductivity in order to minimize the temperature gradients and thus the absolute temperature at the external skin, (3) low density in order to minimize the heating load, (4) mechanical strength compatible with standard operation load, also with extreme loads for safety requirements, (5) machinability in order to produce the exchanger. Beryllium is the best candidate from these points of view.

For the chosen geometry and material, we estimated the exchanger skin temperature and assumed growing of  $SD_2$  along equal-temperature surface (see Fig. 3). Thus, we calculated the shape of the frozen deuterium and the temperature distribution in the bulk of the  $SD_2$  converter under the known  $\gamma$ -heating level.

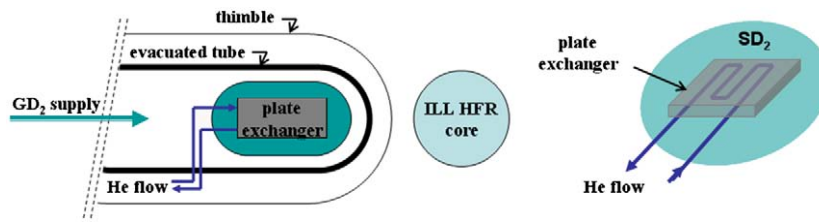


Fig. 2. The heat exchanger principle.

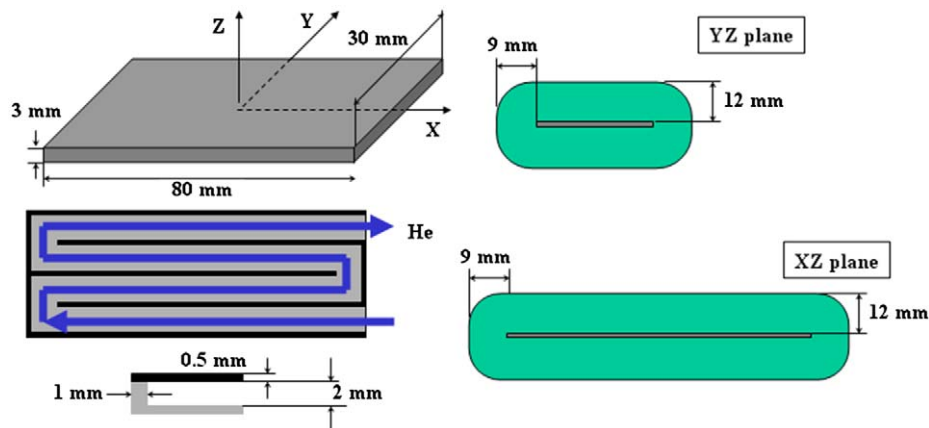


Fig. 3. The considered exchanger geometry and related typical SD<sub>2</sub> converter thickness.

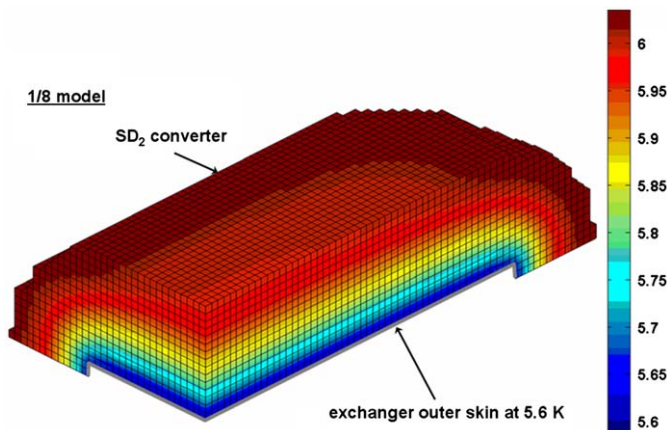


Fig. 4. The temperature distribution in the bulk of a 100 cm<sup>3</sup> converter for a 0.3 W/g heat load.

These studies show that this geometry allows us to keep the SD<sub>2</sub> converter external surface at reasonably low temperature (see Fig. 4).

Finally the required helium flow to evacuate the total heating load (from the exchanger and the converter) was estimated. The exchanger external skin temperature is 5.6 K. In order to minimize the helium flow, the heat exchange coefficient has to be high. This implies high helium flow velocity or small gap between the two conductive plates of the exchanger. As the heat exchange coefficient is only estimated, a safety margin of 2 was applied.

Fig. 5 shows that cooling is feasible, although a large helium flow is needed even for the optimal configuration. The flow pressure drops inside the exchanger; the resistance of the exchanger to the internal pressure of 5 bars is found to be acceptable for the chosen converter design.

So we are going to study experimentally eventual radiation damage for solid deuterium of such a source.

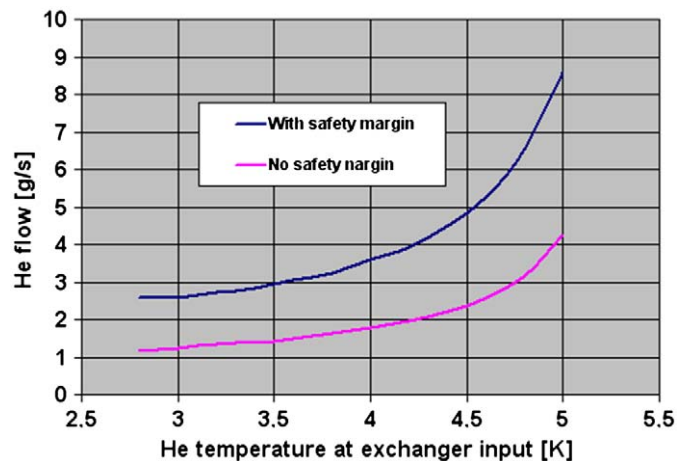


Fig. 5. The required He flow as a function of the input temperature, (1) with no safety margin, and (2) with a safety margin: the theoretical heat exchange coefficient is divided by a factor of 2.

### 3. The experimental setup

The experiment on the irradiation of SD<sub>2</sub> samples was carried out at the MT-25 electron accelerator at the Flerov Laboratory of Nuclear Reactions (FLNR), JINR, Dubna, Russia. We use the electron beam to study the accumulation of energy in SD<sub>2</sub> for the following reasons. An electron beam allows us to irradiate SD<sub>2</sub> with a high rate of absorbed dose, comparable to that foreseen for the UCN SD<sub>2</sub> source at the ILL. At the same time, the radiation dose measured for other materials around the SD<sub>2</sub> sample (cryostat, refrigerator, etc.) is low. The electrons and  $\gamma$ -rays with typical reactor energies produce the same type of radiation damage in deuterium, since the  $\gamma$ -quanta damage results from secondary electrons. The energy of the accelerated electrons was equal to

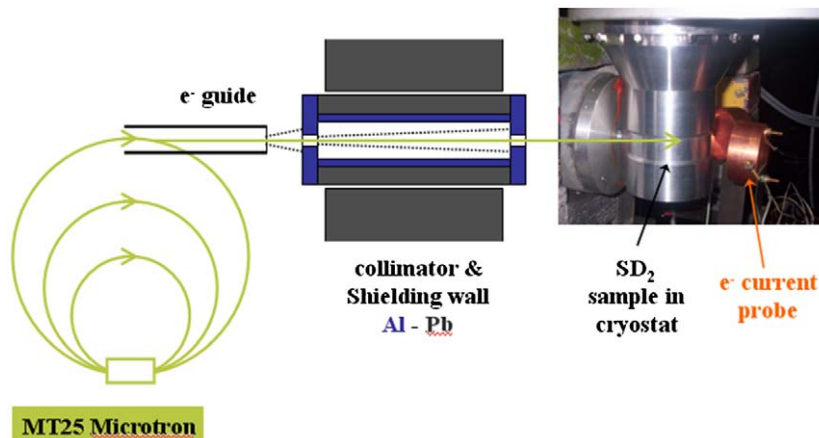


Fig. 6. The electron beam from the electron accelerator MT25 is guided/collimated to the cryostat containing SD<sub>2</sub> sample. The electron current is monitored at the cryostat exit.

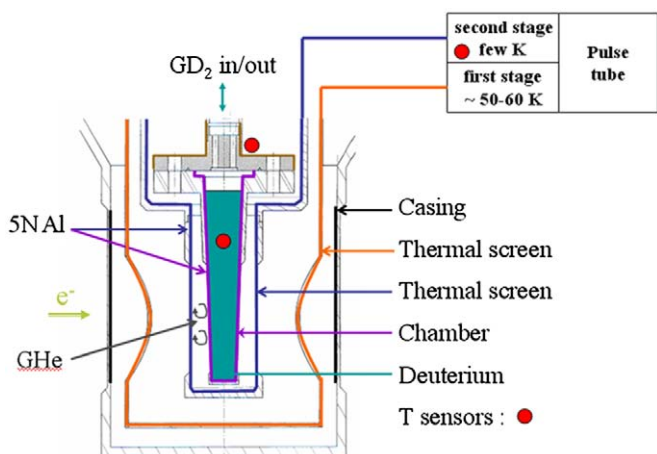


Fig. 7. The cryostat is top-loading. It is cooled by a pulse tube system. Thin windows are manufactured in all the mechanical parts exposed to the electron beam by reducing the thickness of the metal: the external casing, the thermal screens, and the SD<sub>2</sub> sample chamber. The sample is cooled by helium exchange gas situated between the sample chamber and a cold screen connected to the pulse tube cold head (cooling power: 500 mW at 4.2 K, and ~1 W at 5 K).

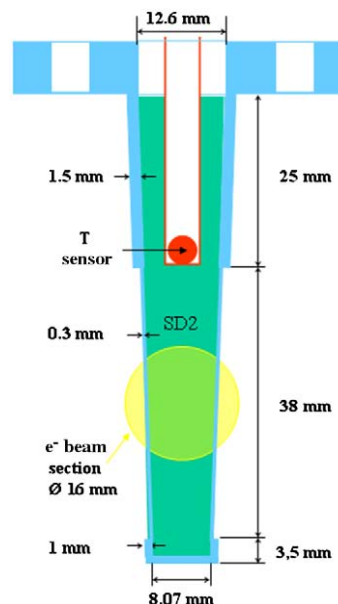


Fig. 8. The SD<sub>2</sub> chamber.

7.8 MeV, sufficiently low to avoid neutron activation of the experimental equipment.

A general view of the experiment is shown in Fig. 6. The cryostat scheme is shown in Fig. 7. The SD<sub>2</sub> sample was produced in two steps. Deuterium gas was first liquefied inside the chamber at a temperature of ~20 K (the gas enters through a capillary tube). The liquid was then solidified by lowering the cryostat temperature to ~3 K. The SD<sub>2</sub> chamber with its temperature sensor is presented in Fig. 8. The thin copper tube is shown in orange; the Teflon flange is indicated in grey.

The SD<sub>2</sub> sample mass was ~1 g; a fraction with a mass of ~0.4 g was exposed to the electron beam. The sample was maintained at a constant temperature in the range 4.2–6.5 K during irradiation with a very low temperature gradient at each temperature.

The collimator length was 200 mm, and the diameter of the round aperture for the electron beam was 10 mm. The collimator protects all cryostat parts from any additional heat load from  $\gamma$ -quanta and electrons in the zones outside the thin windows. It also provides the required electron dose absorption rate of up to 0.5 W/g in the SD<sub>2</sub> sample. A computer simulation of the electron transport was carried out using an MCNP code. This indicated that

the effective electron beam diameter in the SD<sub>2</sub> sample area is equal to ~16 mm. This diameter corresponds to the electron current of 0.8–1  $\mu$ A at the collimator exit. The electron energy was 7.8 MeV (Fig. 8).

The beam probe cup with a diameter of 50 mm and a thickness of 4 mm was made of copper. It covers the dominant fraction of the electron beam at the cryostat exit. The leakage current off the cup was permanently monitored in order to control the energy deposition in the sample. The current off the cup appeared to be equal to only ~45% of the current at the exit of the collimator (both calculated and experimental values). This decrease is caused by the multiple scattering of electrons and the energy loss of electrons passing through the cryostat (mainly through the thick back wall of the outer casing). In order to calibrate the energy deposition, we placed a thin-walled copper tube (0.14 mm)—instead of the sample chamber—inside the cryostat (at room temperature) (see Fig. 9). The energy loss was the same. The change in the temperature of the copper during short irradiation characterizes the energy deposition as a function of the electron current on the cup.

The  $\text{SD}_2$  sample temperature was measured using a Cernox<sup>TM</sup> sensor from LakeShore. This sensor was installed at the end of a thin copper thimble plunging in the  $\text{SD}_2$  sample close to the irradiation zone but outside of it, see Fig. 7. This arrangement allows monitoring small and rapid temperature variations as shown in Fig. 10.

The rise in the  $\text{SD}_2$  sample temperature from  $\sim 3.65$  to  $\sim 3.90$  K in Fig. 10 is due to a sudden change in the sample irradiation level caused by manual adjustment of the electron current. The temperature rise of 0.25 K is clearly detected. This observation confirms the sensitivity of the temperature sensors to small temperature increases, which would occur in case of “burps”. Also it proves high thermal conductivity of the  $\text{SD}_2$  sample, thus negligible difference between the temperature of the irradiation zone and that of the sensor.

#### 4. Sample irradiation and the annealing procedure

The sample was irradiated by an electron beam with energy of 7.8 MeV and an intensity of 0.26–0.8  $\mu\text{A}$  (the current value at the

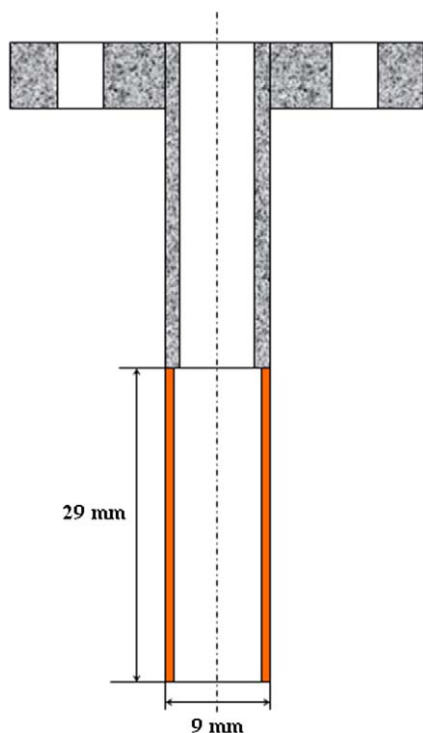


Fig. 9. The chamber mock-up as used for measuring the energy deposition.

collimator exit). The energy deposition in the sample was measured using the calorimetric method described above.

The procedure was as follows. The  $\text{SD}_2$  sample was cooled down to the lowest temperature ( $< 4$  K). The electron beam was then opened and the electron current was adjusted, ensuring that the sample temperature was equal to the desired value in the range 4.2–6.5 K. During irradiation, the temperatures of the  $\text{SD}_2$  sample and the cryostat were continuously recorded at the three points shown in Fig. 2, as was the electron current off the probe.

After a certain period of irradiation, the electron beam was shut down and the electrical power of the special heater at the cryostat cold head was slowly increased stepwise, thus providing a steady rise in the sample temperature. Had there been any release of accumulated energy due to radiolysis, the sample temperature would have risen spontaneously and violently.

#### 5. Results and analysis

##### 5.1. Calibration of the energy deposition in the sample chamber

We carried out two short irradiations of copper mock-up of the sample chamber at the ambient temperature applying maximum electron current of 0.35  $\mu\text{A}$  to the probe cup. The results were corrected using a 2D thermal code to the heat leakage (through the residual air) from the copper tube towards the Teflon flange, the thermocouple, and the screen. The current of 0.35  $\mu\text{A}$  corresponded to the energy deposition of 0.18 W/g in copper, averaged over the 29 mm height of the mock-up (the copper mass of 1 g). Taking into account the difference of (+9%) for linear energy transfer (LET) for the ionized radiation of  $\text{SD}_2$  and copper, we obtained an energy deposition of  $0.20 \pm 0.04$  W/g in a  $\text{SD}_2$  sample with a mass of 0.42 g. An alternative method for estimating the energy deposition would be to use the known dependence of the cold-head temperature on the cryo-cooler cooling power and an estimation of the irradiated mass using a realistic beam profile. The energy deposition is estimated by dividing this cooling power by the total irradiated mass connected to the cold head. This yields a value of  $0.33 \pm 0.10$  W/g, which agrees within experimental uncertainties with that measured using the calorimetric method. The average value was equal to  $0.24 \pm 0.04$  W/g, averaged over the height 29 mm of the  $\text{SD}_2$  sample.

##### 5.2. Stored energy measurement

We carried out five irradiation runs as described in Table 1.

The temperature decrease over five runs was intended to favour storage of the energy; the irradiation duration was adapted each time, to ensure that the total accumulated dose remained representative of the real conditions to be encountered by the  $\text{SD}_2$

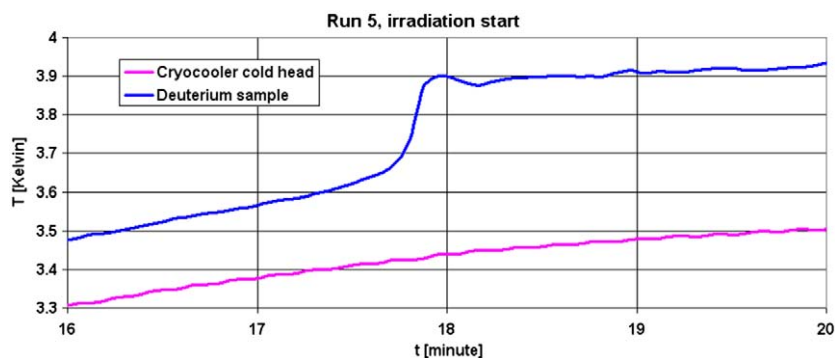


Fig. 10. The evolution of two measured temperatures in case of a sudden change in the irradiation level.

sample inside a high-flux nuclear reactor. No evidence of stored energy release was observed in any of the experimental runs.

The minor fluctuations in temperature shown in Fig. 11 are caused by fluctuations of the electron-beam intensity (recorded simultaneously with the temperature measurements). No other temperature increases were observed. The difference between the absolute temperatures at the cryo-cooler cold-head, the deuterium chamber, and the deuterium sample is explained by the heating effect of the electron beam. The sudden decrease in temperature after about 380 min was caused by a brief interruption in the electron beam.

It is evident from Fig. 12 that a slow steady increase in the sample temperature does not reveal any stored energy in the sample, the three temperatures evolve synchronously.

Consequently, no anomalous temperature variation at the sample was observed. The variations in the cold-head temperature are defined by the consign temperature and the standard cycle of its operation (Fig. 13).

### 5.3. Analysis

The data in Table 1 demonstrate that the characteristic time for energy accumulation in the SD<sub>2</sub> sample due to  $\gamma$ -radiation—if it

occurs at all—is at least longer than the characteristic time of preparation of the SD<sub>2</sub> sample in ILL's potential future UCN SD<sub>2</sub> source. SD<sub>2</sub> sample production close to the reactor active zone is therefore feasible. The maximum characteristic time of the SD<sub>2</sub> sample preparation is estimated to be equal to a fraction of an hour; it is defined by the maximum sample growth rate still providing high transparency of the sample. A source of this type would be operational for some period of time. If this period was comparable to or shorter than the reactor's ~50-day cycle, the sample would need to be periodically renewed.

The sensitivity of the present measurement would allow for undetected temperature jumps of ~0.25 K. We therefore considered the hypothesis of a small undetected temperature increase due to the recombination of radicals. We also considered the operation of a SD<sub>2</sub> source for over 10 h in the ILL reactor in the closest position to the reactor core with the level of  $\gamma$ -radiation corresponding to a heat load of 0.5 W/g (see Fig. 1).

There are three kinds of kinetics possible for the radiation-induced radicals:

- (1) The recombination rate obeys a first-order reaction, where a D-atom would recombine with another from the same "parent" molecule only. This is the most probable case, given

Table 1

	Irradiation duration	Sample temperature (K)	e-current on the probe cup ( $\mu$ A)	Heat deposition in the sample ( $\pm 20\%$ ) (W/g)	Temperature rise due to recombination
1	42 min	6.5–7.2	0.37	0.21	Not detected
2	51 min	6.2–6.5	0.35	0.20	Not detected
3	55 min	4.6–4.8	0.16	0.09	Not detected
4	4 h	4.6–4.9	0.17	0.10	Not detected
5	8 h	4.1–4.4	0.12	0.07	Not detected

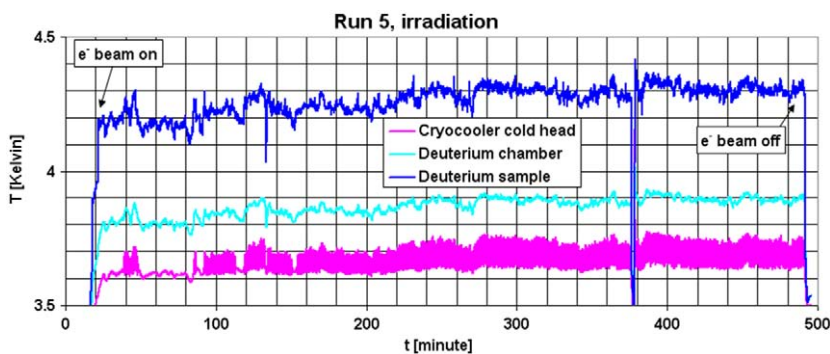


Fig. 11. The values of three recorded temperatures versus time for the longest irradiation period (5th run).

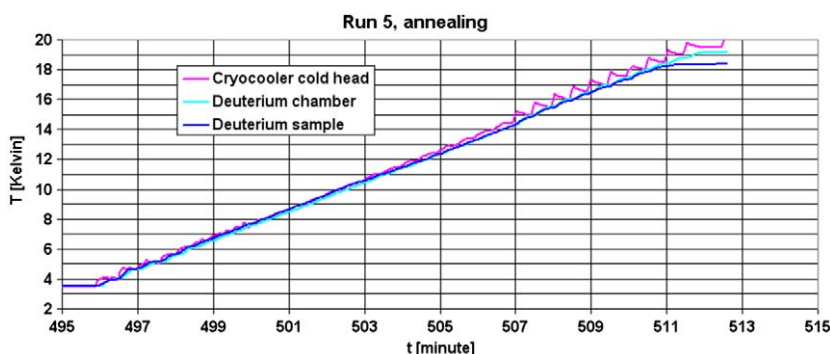


Fig. 12. The evolution of three recorded temperatures during annealing of the SD<sub>2</sub> sample after irradiation.

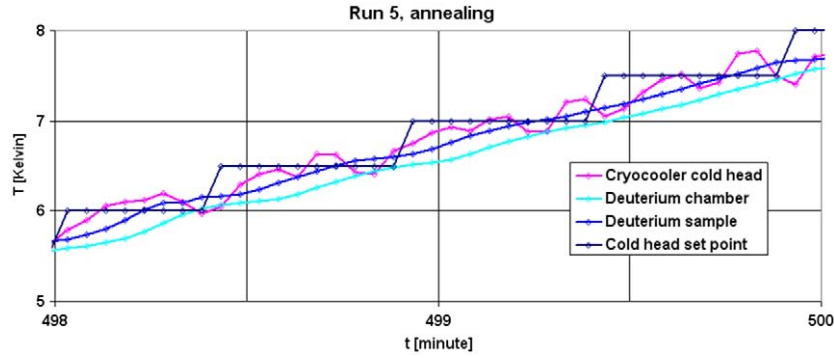


Fig. 13. A “zoom” onto Fig. 6, plus the consign temperature for the automatic regulation of the cold head.

that the LET of the electrons with energy of 8 MeV is as low as 10 meV/nm. Hence, two dissociated molecules (their dissociation energy is 4.55 eV) are far from each other. In addition, the neighbouring deuterium atoms could not survive for long (see Ref. [4]).

- (2) The recombination rate obeys a second-order reaction, where two radicals originate from different molecules located far from each other:

$$\frac{dn_R}{dt} = R - K(T)n_R^2 \quad (1)$$

where  $n_R$  is the radicals' density,  $R$  is their production rate, and  $K(T)$  is small and dependent on the diffusion rate of the radicals.

- (3) In the third case the factor  $K(T)$  is high (radicals' lifetime is short).

We analyze the results in three different ways for these three cases:

- (1) *The recombination rate obeys a first-order reaction.* In this case, the concentration of radicals reaches a saturation value rather fast, and is linearly proportional to their production rate, e.g. to the specific heat deposition. The energy stored (or released during heating)  $Q_{rad}$ , J/mol for a heat deposition rate of 0.5 W/g is estimated as:

$$Q_{rad} = \left( \frac{\delta T C M_{tot}}{M_{irr}} \right) \frac{0.5 \text{ W/g}}{D_{irr}} = (\delta T C M_{tot}) \frac{0.5}{D_{29} M_{29}} \quad (2)$$

where  $\delta T$  is the rise of the  $SD_2$  sample temperature due to the rapid release of stored energy (corresponding to the temperature jump of 0.25 K, which could have stayed undetected), and  $C$  is the specific heat averaged over the temperature interval  $\delta T$ ;  $M_{tot}$ ,  $M_{irr}$ , and  $M_{29}$  are the masses of  $SD_2$  in the sample chamber ( $\sim 1.2$  g), in the irradiated area (unknown), and at the height of 29 mm above the cell bottom (0.42 g), respectively;  $D_{irr}$  and  $D_{29}$  are the specific heat deposition in the area of the beam and that averaged over the height of 29 mm of the sample, respectively. As follows from (2), the beam diameter does not matter in this case. The specific heat value corresponds to a temperature of  $T = 10$ – $11$  K, because molecular the radicals' lifetime shortens at this temperatures. This means that the temperature jumps—if they exist—should happen at a temperature lower than 10–11 K. As the  $C$  value increases as the temperature increases, the choice of a temperature of 10–11 K would maximize the  $Q_{rad}$  estimation. This corresponds to a value  $C \cong 3$ – $4$  J/mol/K. Therefore, the maximum expected energy at a heat deposition rate of 0.5 W/g is

$Q_{rad} \leq 8$  J/mol. The corresponding temperature rise is  $\sim 1.5$  K. An analogous estimation using data on irradiation runs with a 0.37  $\mu$ A electron current provides a value of  $Q_{rad} \leq 3.4$  J/mol. There is a safety margin therefore of at least factor 7 for avoiding sample melting. (A heat deposition of 55 J/mol is required in order to heat the  $SD_2$  sample up to the melting temperature; the melting heat itself is equal to 197 J/mol).

- (2) *The recombination rate obeys the second-order reaction and radical lifetime is long ( $> 10$  h).* This case is close to the previous one, except that it is time-dependent. The estimation for the energy release is equal to  $Q \leq 0.7$  J/mol/h t, where  $t$  is the irradiation time (in hours) at a heating rate of 0.5 W/g. Sample melting might occur after  $\sim 78$  h of continuous irradiation at the temperature of 4.2–4.5 K.
- (3) *The recombination rate obeys the second-order reaction and radical lifetime is short ( $< 3$ – $4$  h).* In this case, the radicals' density was saturated in the experimental run 5. The radicals' saturated density, in accordance with Eq. (1), corresponds to

$$n_R = \sqrt{\frac{\dot{R}}{K(T)}} \quad (3)$$

In the light of this, instead of Eq. (2) we should use another relation

$$Q_{rad} = \frac{(\delta T \bar{C} M_{tot})}{M_{irr}} \sqrt{\frac{0.5 M_{irr}}{D_{29} M_{29}}} \quad (4)$$

(see Eq. (2) for the notations).

In this case, the effective beam size has to be taken into account. It enters as a square root only. On the basis of the beam power balance one can easily obtain an effective beam diameter at the sample of 25–30 mm. (Beam power after the collimator is equal to  $\sim 6.2$  W at the probe cup current of 0.35  $\mu$ A; the power absorbed in the copper mock-up of the sample chamber is equal to  $0.20 \pm 0.04$  W. The beam energy absorbed by the sample chamber is  $\sim 7\%$  according to the MCNP calculation.) Finally, the maximum expected energy release after irradiation at a temperature of 4.2–4.6 K with a heat deposition rate of 0.5 W/g is  $Q_{rad} \leq 7$  J/mol. The corresponding temperature rise is  $\sim 1.0$  K, which is very close to the one obtained above.

#### 5.4. Estimation of the stored energy accumulation under fast neutron radiation

This experiment has allowed us to constrain the accumulation of radicals under electron or gamma radiation. However, there remains the issue of the effect of fast neutrons. A rough semi-empirical estimation could be made on the basis of our experience



with the fast neutron irradiation of other molecular crystals (see Ref. [2]). Let us assume that the rate of accumulation of stored energy in SD<sub>2</sub> is as high as in solid methane (which is the most sensitive to radiation!), e.g. 1.5% of the absorbed dose. Let us also take average neutron energy of 1 MeV. In such a case, the dose rate in the SD<sub>2</sub> would be estimated at  $\sim 0.01$  W/g for a fast neutron flux of  $10^{11}$  n/cm<sup>2</sup>/s. The rate of stored energy accumulation in the SD<sub>2</sub> is  $1.5 \times 10^{-4}$  W/g. If the radicals' lifetime is  $> 10$  h, the stored energy would be equal to  $\sim 22$  J/mol after 10 h of fast neutron irradiation. This is equivalent to a temperature rise of 9 K. Keeping in mind the hypothesis considered, this yields an upper constraint for the temperature rise. Consequently SD<sub>2</sub> melting might occur under fast neutron irradiation of a duration exceeding 25 h.

Another question that will need to be addressed is the effect of the thermal conductivity of ortho-deuterium on the rate of dissociation of molecules and the recombination of radicals as compared to solid methane.

## 6. Conclusion

The results obtained provide assurance that the maximum expected stored energy release in the SD<sub>2</sub> ILL source would not exceed 7 J/mol after 10 h of  $\gamma$ - or electron irradiation at a temperature of 4.2–4.6 K and a heat deposition of 0.5 W/g. This corresponds to a temperature rise of  $\sim 1.5$  K. For an irradiation temperature of 6–6.5 K, the energy release would be lower. A safety factor of at  $\geq 7$  assures against sudden melting of SD<sub>2</sub>. Rough theoretical estimations of the influence of fast neutrons show that the stored energy would be  $< 22$  J/mol after irradiation with a flux of  $\sim 10^{11}$  n/cm<sup>2</sup>/s of fast neutrons during 10 h. This is equivalent to a temperature rise of  $\sim 9$  K. We conclude that the phenomenon of energy accumulation in SD<sub>2</sub> under irradiation would not present an obstacle to the construction of a SD<sub>2</sub> UCN source positioned within the highest neutron fluxes available at the ILL reactor. If burps in SD<sub>2</sub> would occur at a time scale longer than that studied here, the source could be operated in a cyclic mode, i.e. one could imagine to regularly (for instance, once per few hours) warm the SD<sub>2</sub> crystal to  $\sim 10$  K. This way, any radicals and stored energy at 5 K could be released. More detailed studies are needed to optimize the design and operating regime of such a source.

## Acknowledgements

This work was carried out in the framework of the contract "Accomplishment of experiments on irradiation of solid deuterium by electrons at the MT-25 microtron of JINR". We would like to thank LPSC, Grenoble, France, for its kind support with the manufacture of specialised cryostat components, and also A.G. Belov, E.V. Lychagin, A.Yu. Muzychka, A.V. Strelkov for their help during the measurements.

## References

- [1] V. Shevtsov, et al., *J. Low Temp. Phys.* 95 (5/6) (1994) 1.
- [2] E. Shabalin, in: *Proceedings of the Workshop on Cold Moderators for Pulsed Neutron Sources*, Argonne, Illinois, ANL, 28 September–2 October 1997, ANL-Report, 1998.
- [3] E. Shabalin, et al., *Radiat. Phys. Chem.* 67 (3–4) (2003) 315.
- [4] E. Kulagin, et al., *Nucl. Instr. and Meth. B* 215 (1–2) (2004) 181.
- [5] R. Golub, M.J. Pendlebury, *Phys. Lett. A* 53 (1975) 133.
- [6] R. Golub, K. Boning, *Zeit. Phys. B* 51 (1983) 95.
- [7] R. Golub, *Nucl. Instr. and Meth. A* 226 (1984) 2.
- [8] A.P. Serebrov, et al., *JETP Lett.* 59 (1994) 757.
- [9] A.P. Serebrov, et al., *JETP Lett.* 62 (1995) 785.
- [10] U. Trinks, et al., *Nucl. Instr. and Meth. A* 440 (2000) 666.
- [11] R.E. Hill, et al., *Nucl. Instr. and Meth. A* 440 (2000) 717.
- [12] A.P. Serebrov, et al., *Nucl. Instr. and Meth. A* 440 (2000) 658.
- [13] A.P. Serebrov, et al., *JETP Lett.* 74 (2001) 302.
- [14] C.L. Morris, et al., *Phys. Rev. Lett.* 89 (2002) 272501.
- [15] F. Atchison, et al., *Phys. Rev. B* 68 (2003) 094114.
- [16] A. Saunders, et al., *Phys. Lett. B* 593 (2004) 55.
- [17] F. Atchison, et al., *Phys. Rev. C* 71 (2005) 054601.
- [18] A. Frei, et al., *EPJ A* 34 (2007) 119.
- [19] F. Atchison, et al., *Phys. Rev. Lett.* 99 (2007) 262502.
- [20] Korobkina, et al., *Nucl. Instr. and Meth. A* 579 (2007) 530.
- [21] I. Altarev, et al., *EPJ A* 37 (2008) 9.
- [22] I. Altarev, et al., *Phys. Rev. Lett.* 100 (2008) 014801.
- [23] F. Atchison, et al., *Phys. Rev. Lett.* 101 (2008) 189902.
- [24] H. Soerensen, *Appl. Phys.* 9 (1976) 321.
- [25] G. Rosen, *J. Chem. Phys.* 65 (1976) 1735.
- [26] R.L. Brooks, et al., *Phys. Rev. Lett.* 51 (12) (1983) 1077.
- [27] R.L. Brooks, et al., *Phys. Rev. B* 32 (4) (1985) 2478.
- [28] T. Miyazaki, et al., *Chem. Phys. Lett.* 182 (1) (1991) 35.
- [29] G.W. Collins, et al., *Phys. Rev. B* 45 (2) (1992) 549.
- [30] J.A. Forrest, et al., *Phys. Rev. B* 50 (13) (1994) 9573.
- [31] J.A. Forrest, et al., *Phys. Rev. B* 55 (2) (1997) 906.
- [32] V.V. Nesvizhevsky, *Nucl. Instr. and Meth. A* 557 (2006) 576.
- [33] C. Plonka, et al., *Nucl. Instr. and Meth. A* 578 (2007) 450.
- [34] V.V. Nesvizhevsky, et al., *Nucl. Instr. and Meth. A* 578 (2007) 435.
- [35] V.V. Nesvizhevsky, et al., *Nature* 415 (2002) 297.
- [36] V.V. Nesvizhevsky, K.V. Protasov, in: *Edited Book on Trends in Quantum Gravity Research*, NOVA, New York, 2006, pp. 65–107.